

# ErAs/InGaAs superlattice Seebeck coefficient

Gehong Zeng, John E. Bowers

Department of Electrical and Computer Engineering, University of California, Santa Barbara, CA 93106

Yan Zhang, and Ali Shakouri\*

Electrical Engineering Department, University of California-Santa Cruz , 1156 High Street, Santa Cruz, CA 95064

Joshua Zide, Arthur Gossard

Materials Department, University of California, Santa Barbara, CA 93106

Woochul Kim, Arun Majumdar

Department of Mechanical Engineering, University of California, Berkeley, CA 94720

\*Corresponding Email: ali@soe.ucsc.edu, phone: (831) 459-3821

## Abstract

InGaAs with embedded ErAs nano-particles is a promising material for thermoelectric applications. The incorporation of erbium arsenide metallic nanoparticles into the semiconductor can provide both charge carriers and create scattering centers for phonons. Electron filtering by heterostructure barriers can also enhance Seebeck coefficient by selective emission of hot electrons. 2.1 $\mu\text{m}$ -thick ErAs/InGaAs superlattices with a period of 10 nm InAlGaAs and 20 nm InGaAs were grown using molecular beam epitaxy, and the effective doping is from  $2 \times 10^{18}$  to  $1 \times 10^{19} \text{ cm}^{-3}$ . Special device patterns were developed for the measurement of the cross-plane Seebeck coefficient of the superlattice layers. Using these device patterns, the combined Seebeck coefficient of superlattice and the substrate were measured and the temperature drops through the superlattice and InP substrate were determined with 3D ANSYS<sup>®</sup> simulations. The Seebeck coefficient of the superlattice layers is obtained based on the measurements and simulation results.

## Introduction

The Seebeck coefficient of thermoelectrical material is of great importance for thermoelectrical devices working either as coolers or generators. For TE coolers, the cooling power is proportional to the Seebeck coefficient of the element material, and the output power of thermal-to-electricity power generator is proportional to the square of the Seebeck coefficient.

Superlattice structure can enhance thermoelectrical device performance by the selective emission of hot carriers above the barrier layer through thermionic emissions<sup>1</sup>. And the figure of merit ZT of a semiconductor can also be improved

by incorporating of semi-metallic nano-particles into the material to form phonon scattering centers and increase carrier concentration<sup>2</sup>. The metal-based superlattices with tall barriers can achieve a large effective thermoelectric figure of merit by electron filtering<sup>3</sup>. In-plane and cross-plane Seebeck coefficient for superlattices are usually different, mainly because of filtering effects. The in-plane Seebeck coefficient measurement is straightforward: building up a temperature difference across the sample and measuring the output voltage. By comparison, the measurements of cross-plane Seebeck coefficient are more obscure, for the temperature difference across superlattice layer of a few microns can not be directly measured precisely. In our previous work, we used the same device pattern and measured SiGe/Si superlattice cross-plane Seebeck coefficients<sup>4</sup>. In this paper, we report the measurements of cross-plane Seebeck coefficients of ErAs/InGaAs superlattices.

## Materials Growth and Structure

Four ErAs/InGaAs superlattice samples were grown using a Varian Gen II molecular beam epitaxy system on (100) n-type InP substrate. The samples have the superlattice structure. Erbium particles are randomly distributed through InGaAs layers, which provide  $2 \times 10^{18} \text{ cm}^{-3}$  doping. Silicon co-doping for the four superlattice samples are 0,  $2 \times 10^{18}$ ,  $4 \times 10^{18}$  and  $8 \times 10^{18} \text{ cm}^{-3}$ , thus the effective doping of erbium and silicon dopants for the four samples are  $2 \times 10^{18}$ ,  $4 \times 10^{18}$ ,  $6 \times 10^{18}$  and  $8 \times 10^{18} \text{ cm}^{-3}$  respectively. The structure of superlattice is illustrated in Figure 1 and the compositions of the four samples are shown in table 1.

**Table 1:** Four ErAs/InGaAs superlattice samples have structure with different silicon co-doping.

	Superlattice structure	Effective doping ( $\text{cm}^{-3}$ )
1	70 $\times$ (10nm (InGaAs) <sub>0.6</sub> (InAlAs) <sub>0.4</sub> /20nm (n-InGaAs) <sub>0.997</sub> Er <sub>0.003</sub> randomly)	$2 \times 10^{18}$
2	70 $\times$ (10nm (InGaAs) <sub>0.6</sub> (InAlAs) <sub>0.4</sub> /20nm (n-InGaAs) <sub>0.997</sub> Er <sub>0.003</sub> randomly, $2 \times 10^{18}$ Si)	$4 \times 10^{18}$
3	70 $\times$ (10nm (InGaAs) <sub>0.6</sub> (InAlAs) <sub>0.4</sub> /20nm (n-InGaAs) <sub>0.997</sub> Er <sub>0.003</sub> randomly, $4 \times 10^{18}$ Si)	$6 \times 10^{18}$
4	70 $\times$ (10nm (InGaAs) <sub>0.6</sub> (InAlAs) <sub>0.4</sub> /20nm (n-InGaAs) <sub>0.997</sub> Er <sub>0.003</sub> randomly, $8 \times 10^{18}$ Si)	$1 \times 10^{19}$

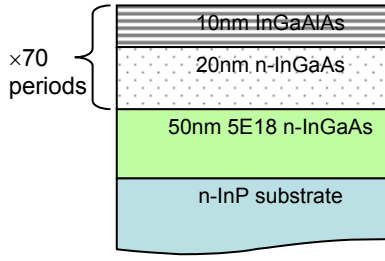


**Figure 1:** Schematic of device structure

### Device fabrication

We fabricated the test patterns both on superlattice and substrate. The device was fabricated with first forming a  $3\mu\text{m}$ -mesa by etching the superlattice layer down to the InP substrate using reactive ion etching. Ni/GeAu/Ni/Au layers were used as contact metal on both n and p type ErAs/InGaAs superlattice on the top of the mesa and InP substrate at the bottom of the mesa.  $1\mu\text{m}$ -thick Ti/Au heater wires were formed on top of contact area. The heater wire and contact metal layer were isolated using  $300\text{ nm}$   $\text{SiO}_2/\text{SiN}$  double layers. As devices sit both on top of the superlattice mesa and on the substrate, cross-plane Seebeck of the superlattice and the Seebeck of bulk InP substrate can be measured using these devices. Figure 2 is the CCD picture of these Seebeck measurement devices. Figure 3 illustrates the measurement set-up.

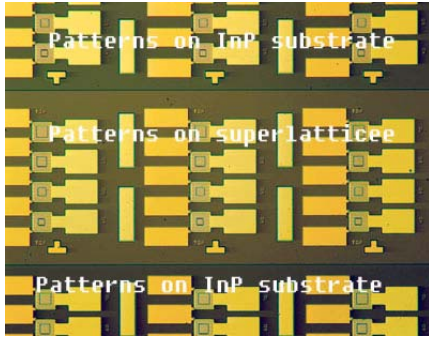


**Figure 2:** Seebeck measurement devices sitting on both top of the  $3\mu\text{m}$  superlattice mesa and on the InP substrate respectively.

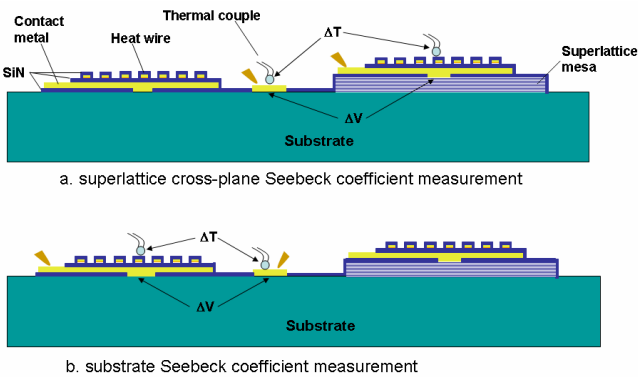


**Figure 3:** Schematic of Seebeck coefficient measurement set-up

### Results and Discussions

The measurement of bulk Seebeck for the InP is straight forward using the devices sitting on the InP substrate. When current was applied through the device heater wire, there's a temperature rise beneath the wire area. By measuring the temperature difference  $\Delta T$  and voltage output  $\Delta V$  between this heater wire point and another metal contact, the Seebeck coefficient  $\alpha = \Delta V/\Delta T$  can be known. Figure 4 shows the measurement results.

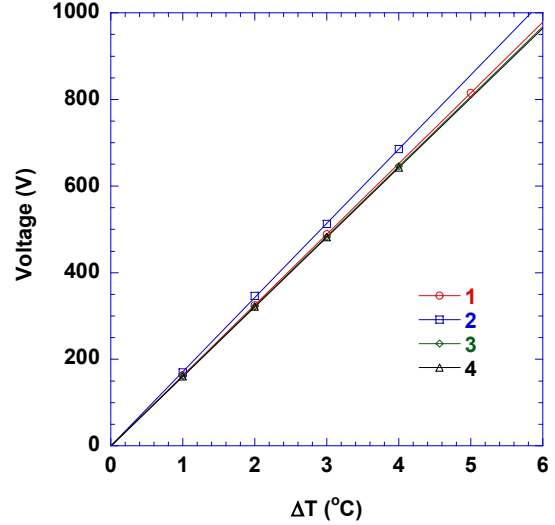


**Figure 4:** Measured results for InP substrate of sample 1, 2, 3 and 4 respectively using device patterns.

The Seebeck coefficients for the four samples from #1 to #4 were measured as  $162.96\ \mu\text{V/K}$ ,  $171.40\ \mu\text{V/K}$ ,  $161.35\ \mu\text{V/K}$  and  $160.70\ \mu\text{V/K}$  respectively using devices sitting on the InP substrate. When one device sitting on top of the superlattice and one electrode on the InP substrate are used for the measurement, the results are the combination from both  $2.1\ \mu\text{m}$  superlattice and InP substrate. This combinational Seebeck coefficient,  $\alpha_{\text{combo}}$  can be described as  $\alpha_{\text{combo}}\Delta T = \alpha_{\text{SL}}\Delta T_{\text{SL}} + \alpha_{\text{sub}}\Delta T_{\text{sub}}$ , where  $\Delta T$  is the total temperature dropping from the top of the superlattice to the InP substrate,  $\Delta T_{\text{SL}}$  and  $\Delta T_{\text{sub}}$  are the temperature dropping across the superlattice and InP substrate respectively;  $\alpha_{\text{SL}}$  is cross-plane Seebeck coefficient of the superlattice, and  $\alpha_{\text{sub}}$  the InP substrate Seebeck coefficient, and the temperature relationship is  $\Delta T = \Delta T_{\text{SL}} + \Delta T_{\text{sub}}$ . The measurement results of the combination Seebeck coefficient for sample 1, 2, 3 and 4 are shown in figure 3 and the measurement results of combinational Seebeck coefficients are  $284.14\ \mu\text{V/K}$ ,  $248.72\ \mu\text{V/K}$ ,  $213.55\ \mu\text{V/K}$  and  $196.95\ \mu\text{V/K}$  for samples 1, 2, 3 and 4 respectively.

In our device patterns for the cross-plane Seebeck measurement, the values of  $\Delta T$ ,  $\Delta V$  and  $\alpha_{\text{sub}}$  are measured directly, where  $\Delta V$  is the output voltage at the two points with temperature difference  $\Delta T$ . The voltage  $\Delta V$  can be expressed as  $\Delta V = \alpha_{\text{SL}}\Delta T_{\text{SL}} = \alpha_{\text{sub}}\Delta T_{\text{sub}}$ , and the  $\alpha_{\text{SL}}$  can be known only when the temperature dropping  $\Delta T_{\text{SL}}$  or  $\Delta T_{\text{sub}}$  or the ratio  $\Delta T_{\text{SL}}/\Delta T_{\text{sub}}$  is know. Figure 4 shows that calculation of

Seebeck coefficient value for different temperature dropping ratio  $\Delta T_{SL}/\Delta T$ .

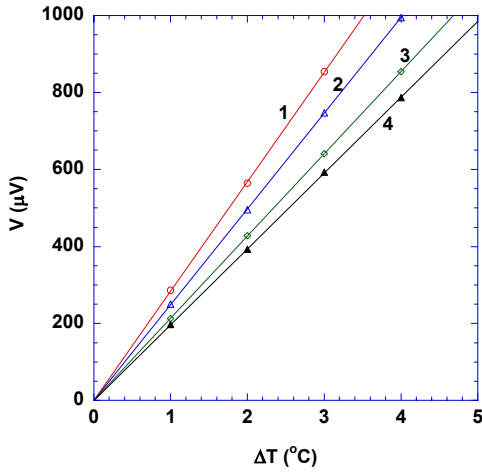


**Figure 5:** The measurement results of combinational Seebeck for samples 1, 2, 3 and 4

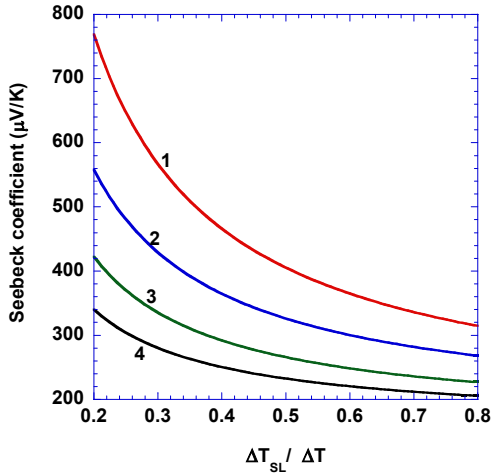


**Figure 6:** Cross-plane Seebeck coefficient calculation values for sample 1, 2, 3, and 4, based on the measurements of  $\Delta T$ ,  $\Delta V$ ,  $\alpha_{sub}$  and the relationship of  $\Delta V = \alpha_{SL}\Delta T_{SL} = \alpha_{sub}\Delta T_{sub}$  and  $\Delta T = \Delta T_{SL} + \Delta T_{sub}$

3D thermal simulations were carried out to find the temperature difference ratio of  $\Delta T_{SL}/\Delta T$  using ANSYS® multiphysics module. As the Seebeck coefficient measurements are static, no other thermal effects, such as Peltier or Thomson, will occur. The thermal properties needed to know for the simulations are material thermal conductivities. In our experiments, the thermal conductivities of ErAr/InGaAs, SiO<sub>2</sub>, and SiN were measured using  $3\omega$  method<sup>5,6</sup>. Our thermal simulation results show that the temperature difference ratio of  $\Delta T_{SL}/\Delta T$  for our devices is around 0.5, thus the cross-plane Seebeck coefficients for sample 1, 2, 3 and 4 are 405.32  $\mu\text{V/K}$ , 326.04  $\mu\text{V/K}$ , 265.75  $\mu\text{V/K}$  and 232.40  $\mu\text{V/K}$  respectively.

As the above measurements were on device patterns, which assume that the temperature measured on top of the

heater wires is very close to the temperature at the superlattice/metal interface, so the Seebeck coefficients of the InP substrates for sample 1, 2, 3 and 4 were re-measured for calibrations: the 520  $\mu\text{m}$  strip samples were lapping down at the superlattice surface to 470  $\mu\text{m}$  to totally remove the superlattice, then the sample was placed on two thermoelectrical coolers which were set at two different temperatures  $T_1$  and  $T_2$ . The voltage and temperature at the two ends of the sample was measured with a multimeter and two thermal couples simultaneously. The diagram of measurement setup is shown in figure 7.

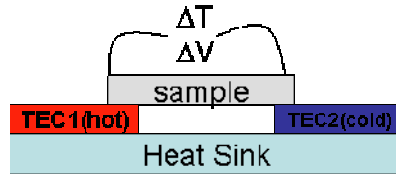


**Figure 7:** Schematic diagram for the Seebeck coefficient measurement of InP substrate.

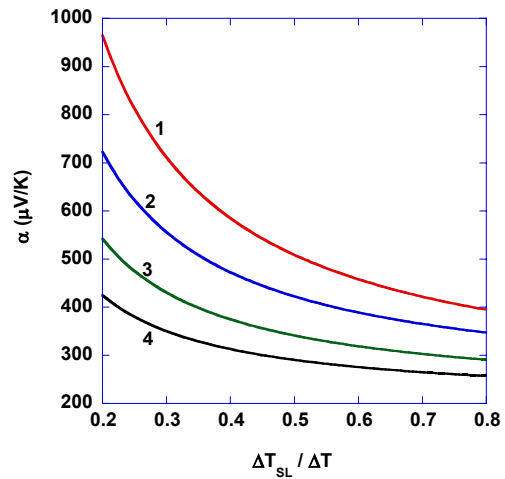


**Figure 8:** Cross-plane Seebeck coefficient calculation values after calibrations for sample 1, 2, 3, and 4, based on the measurements in figure 3.

As the above measurement is straight forward, it was used as a calibration for device pattern measurements. The measured Seebeck coefficient values are 204.49  $\mu\text{V/K}$ , 221.98  $\mu\text{V/K}$ , 207.08  $\mu\text{V/K}$  and 200.82  $\mu\text{V/K}$  for the InP substrate of sample 1, 2, 3 and 4 respectively.

By comparing results in two methods, there's a difference of 0.2031, 0.2279, 0.2209 and 0.1998 between the two measurements for sample 1, 2, 3 and 4 respectively. The device pattern measurement result values are about 20% less than those using two thermoelectric cooler setup. The reason for these is that the temperatures measured using device patterns were about 20% higher than the real temperatures at the InP/metal interfaces. The differences of 0.2031, 0.2279, 0.2209 and 0.1998 were used as calibration factor for the combinational Seebeck coefficient results shown in figure 3

using device patterns. The figure 8 shows the cross-plane Seebeck coefficient values after the calibrations. The Seebeck coefficients are 508.61  $\mu\text{V/K}$ , 422.25 $\mu\text{V/K}$ , 341.07 $\mu\text{V/K}$  and 290.42 $\mu\text{V/K}$  when the temperature ratio of  $\Delta T_{\text{SL}}/\Delta T$  is 0.5.

### Conclusions

Four ErAs/InGaAs superlattice samples were grown using molecular beam epitaxy with different silicon doping levels. Devices were fabricated and the combinational Seebeck coefficients were measured. The temperature ratio of  $\Delta T_{\text{SL}}/\Delta T$  for the devices was determined with ANSYS<sup>®</sup> simulations. The InP substrates of the samples were measured using thermoelectric cooler setup for calibrations. The cross-plane Seebeck coefficients of the ErAs/InGaAs superlattices for the four samples 1, 2, 3 and 4 are 508.61  $\mu\text{V/K}$ , 422.25  $\mu\text{V/K}$ , 341.07  $\mu\text{V/K}$  and 290.42  $\mu\text{V/K}$ , respectively.

### Acknowledgments

This work is supported by the Office of Naval Research Thermionic Energy Conversion Center MURI monitored by Dr. Mihal E. Gross.

### References

- <sup>1</sup> A. Shakouri and J. E. Bowers, Applied Physics Letters 71, 1234-1236 (1997).
- <sup>2</sup> D. G. Cahill, W. K. Ford, K. E. Goodson, G. D. Mahan, A. Majumdar, H. J. Maris, R. Merlin, and S. R. Phillpot, Journal of Applied Physics 93, 793-818 (2003).
- <sup>3</sup> D. Vashaee and A. Shakouri, Physical Review Letters 92, 106103/1 (2004).
- <sup>4</sup> Y. Zhang, G. Zeng, R. Singh, J. Christofferson, E. Croke, J. E. Bowers, and A. Shakouri, Measurement of Seebeck coefficient perpendicular to SiGe Superlattice, 329-331 (2002).
- <sup>5</sup> D. G. Cahill, Review of Scientific Instruments 61, 802-808 (1990).
- <sup>6</sup> D. G. Cahill, H. E. Fischer, T. Klitsner, E. T. Swartz, and R. O. Pohl, Journal of Vacuum Science & Technology a- Vacuum Surfaces and Films 7, 1259-1266 (1989).